New Phytologist

The *TuMYB46L-TuACO3* module regulates ethylene biosynthesis in einkorn wheat defense to powdery mildew

Hongyuan Zheng[1,2]*, Lingli Dong[2]*, Xinyun Han[2], Huaibing Jin[2], Cuicui Yin[3], Yali Han[2], Bei Li[2,4], Huanju Qin[2], Jinsong Zhang[3,4], Qianhua Shen[2,4], Kunpu Zhang[2] and Daowen Wang[2,4,5]

[1]College of Agronomy, Henan Agricultural University, Zhengzhou 450002, China; [2]The State Key Laboratory of Plant Cell and Chromosome Engineering, Institute of Genetics and Developmental Biology, Chinese Academy of Sciences, Beijing 100101, China; [3]The State Key Laboratory of Plant Genomics, Institute of Genetics and Developmental Biology, Chinese Academy of Sciences, Beijing 100101, China; [4]University of Chinese Academy of Sciences, Beijing 100049, China; [5]The State Key Laboratory of Wheat and Maize Crop Science, Henan Agricultural University, Zhengzhou 450002, China

Authors for correspondence:
Daowen Wang
Tel: +86 10 64806575
Email: dwwang@genetics.ac.cn

Kunpu Zhang
Tel: +86 10 64806576
Email: zkp66@126.com

Received: *30 July 2019*
Accepted: *22 October 2019*

New Phytologist (2020) **225:** 2526–2541
doi: 10.1111/nph.16305

Key words: ACC oxidase (ACO), *Blumeria graminis*, einkorn wheat, ethylene (ET), gene module, MYB transcription factor, plant defense.

Summary

- Powdery mildew disease, elicited by the obligate fungal pathogen *Blumeria graminis* f.sp. *tritici* (*Bgt*), causes widespread yield losses in global wheat crop. However, the molecular mechanisms governing wheat defense to *Bgt* are still not well understood.
- Here we found that *TuACO3*, encoding the 1-aminocyclopropane-1-carboxylic acid (ACC) oxidase functioning in ethylene (ET) biosynthesis, was induced by *Bgt* infection of the einkorn wheat *Triticum urartu*, which was accompanied by increased ET content. Silencing *TuACO3* decreased ET production and compromised wheat defense to *Bgt*, whereas both processes were enhanced in the transgenic wheat overexpressing *TuACO3*.
- TuMYB46L, phylogenetically related to *Arabidopsis* MYB transcription factor AtMYB46, was found to bind to the *TuACO3* promoter region in yeast-one-hybrid and EMSA experiments. *TuMYB46L* expression decreased rapidly following *Bgt* infection. Silencing *TuMYB46L* promoted ET content and *Bgt* defense, but the reverse was observed when *TuMYB46L* was overexpressed.
- Hence, decreased expression of *TuMYB46L* permits elevated function of *TuACO3* in ET biosynthesis in *Bgt*-infected wheat. The *TuMYB46L-TuACO3* module regulates ET biosynthesis to promote einkorn wheat defense against *Bgt*. Furthermore, we found four chitinase genes acting downstream of the *TuMYB46L-TuACO3* module. Collectively, our data shed a new light on the molecular mechanisms underlying wheat defense to *Bgt*.

Introduction

Common wheat (*Triticum aestivum*, AABBDD) is the most widely cultivated staple crop in the world (IWGSC *et al.*, 2018). Efficient and stable wheat production is essential for maintaining global food security. Powdery mildew disease, caused by the obligate biotrophic fungal pathogen *Blumeria graminis* f.sp. *tritici* (*Bgt*), leads to widespread yield reductions in many wheat-producing regions (Singh *et al.*, 2016). The infection cycles of cereal powdery mildew fungi (including *Bgt*) are similar to each other (Hückelhoven & Panstruga, 2011; Wicker *et al.*, 2013). Under favorable conditions, the conidium germinates and produces a primary germ tube and an appressorial germ tube (AGT). The AGT then develops into an appressorium from which an infection peg emerges. In a compatible interaction, the infection peg enters host cells and forms a haustorium. This structure absorbs nutrients from host cells and promotes rapid secondary hyphae growth on the leaves, leading to the formation of powdery mildew colonies and the production of a new generation of conidia. To manage the damages inflicted by *Bgt*, substantial efforts are being devoted to study the genetic and molecular mechanisms of wheat defense to powdery mildew disease in order to develop effective controlling measures (Yahiaoui *et al.*, 2004; Bhullar *et al.*, 2010; He *et al.*, 2018; McNally *et al.*, 2018; Xing *et al.*, 2018; Zou *et al.*, 2018).

To date, two layers of plant immunity to pathogen attacks have been elucidated (Bigeard *et al.*, 2015; Cui *et al.*, 2015). Pattern triggered immunity (PTI), initiated by recognition of pathogen associated molecular patterns by host cell surface receptors, is a basal level of defense. However, effector triggered immunity (ETI), augmented after detecting the avirulent effector of pathogen by host intracellular immunoreceptor molecules, is an intensified form of defense often with high race specificity. Many defense proteins, such as various types of pathogen-related (PR) proteins including chitinases, are induced upon the activation of PTI and ETI, and contribute

*These authors contributed equally to this work.

to the limitation of pathogen growth. The mechanisms underlying the induction of defense genes are highly complex, which frequently involve phytohormone signaling processes and vary among different pathosystems (Pieterse *et al.*, 2012; Bigeard *et al.*, 2015; Cui *et al.*, 2015). Detailed characterization of these mechanisms is essential for completely understanding the genetic and molecular basis of plant defense to different pathogen attacks.

Through molecular and genetic analysis, ethylene (ET) biosynthesis and signal transduction have been found to regulate plant defense to diverse pathogens (Broekaert *et al.*, 2006; Tintor *et al.*, 2013; Broekgaarden *et al.*, 2015). In *Arabidopsis thaliana*, ET biosynthesis was activated in response to the infection by the necrotroph *Botrytis cinerea* (Gravino *et al.*, 2015); ET induction also was shown to play a positive role in defense against the bacterial pathogen *Pseudomonas syringae* pv. *tomato* DC3000 (Guan *et al.*, 2015). In both studies, the infection-induced ET biosynthesis was caused by increased activity of 1-aminocyclopropane-1-carboxylic acid synthase (ACS), a key enzyme required for ET biosynthesis in plant cells (Booker & Delong, 2015). In line with the above findings, a recent work shows that rice defense against the hemi-biotrophic fungal pathogen *Magnaporthe oryzae* also involved the upregulation of ET production through the function of ACS. Apart from ACS, several transcriptional factor (TF) genes acting in the ET signaling pathway also have been demonstrated to regulate plant defense against pathogens. TaPIE1, a pathogen-induced ET responsive factor (ERF), was reported to positively regulate the resistance response to *Rhizoctonia cerealis* by activating the transcription of defense-related genes downstream of the ET signaling pathway (Zhu *et al.*, 2014). Overexpression of *GmERF5* was shown to enhance the resistance of soybean to *Phytophthora sojae* via positively regulating the expression of the defense genes *PR10*, *PR1-1* and *PR10-1* (Dong *et al.*, 2015a). Activation of two TFs functioning in ET signaling in rice increased the resistance to *M. oryzae* by elevating the production of reactive oxygen species (ROS) and phytoalexins (Yang *et al.*, 2017). Finally, ectopic expression of *ERF1-V*, an ET-responsive element-binding factor gene of the AP2/ERF transcription factor gene family, conferred high resistance to *Bgt* infection in wheat (Xing *et al.*, 2017). Despite the progress outlined above, there is still little molecular evidence for the function of ET biosynthesis and signaling in plant defense to obligate biotrophic fungal pathogens, such as powdery mildew fungi.

Higher plants generally possess a large family of MYB TF genes, many of which have been found to regulate plant defense against pathogens. For example, the knockout of AtMYB46, an R2R3 type MYB TF originally found to regulate secondary cell wall biosynthesis in *Arabidopsis* (Zhong *et al.*, 2007; Zhong & Ye, 2012), confers enhanced resistance to *B. cinerea* through increasing the expression of cell wall remodeling genes encoding type III peroxidases and two defense-related genes coding for PR3 and PDF1.2a (Ramírez *et al.*, 2011a,b). Another *Arabidopsis* R2R3 MYB TF, *MYB15*, positively regulates *Arabidopsis* basal immunity to the bacterial pathogen *Pseudomonas syringae* through promoting defense-induced lignification (Chezem *et al.*, 2017). *MYBS1*, a MYB TF gene in rice, contributes to rice defense against *M. oryzae* through suppressing *bsr-d1* gene expression, which resulted in elevated ROS accumulation and, thus, limited pathogen growth (W. Li *et al.*, 2017). Finally, several MYB TF genes inducible by ET treatment, including *MYB108* from cotton, and *TaMYB4* and *TaPIMP2* from wheat (Al-Attala *et al.*, 2014; Cheng *et al.*, 2016; Wei *et al.*, 2017), are found to contribute to plant defense against pathogens. Nevertheless, there is still no detailed report on the regulation of plant pathogen defense by MYB TFs through upregulating the transcription of ET biosynthesis gene(s) and the resultant elevation of ET production.

In order to efficiently analyze the defense mechanisms to *Bgt*, we used the diploid einkorn wheat *Triticum urartu* (AA), which has a much smaller genome than that of common wheat, as an experimental host (Zhang *et al.*, 2016; Ling *et al.*, 2018). *Triticum urartu* accessions from around the world differed extensively in their response to *Bgt* infection; *T. urartu* genes and networks associated with different types of resistance responses to *Bgt* have been revealed by transcriptome comparison and selection sweep mapping analyses (Zhang *et al.*, 2016; Ling *et al.*, 2018). Further to the studies above, we here report the function of *TuACO3* and *TuMYB46L*, encoding an active 1-aminocyclopropane-1-carboxylic acid (ACC) oxidase (ACO) enzyme and a R2R3 myeloblastosis (MYB) TF, respectively, in wheat defense against *Bgt*. We found that the expression of *TuACO3* was increased by *Bgt* infection in diverse *T. urartu* accessions, and its protein promoted ET biosynthesis in *Bgt*-infected plants. Silencing *TuACO3* lowered *Bgt* infection-induced ET production and weakened the defense against *Bgt*. Through yeast-one-hybrid (Y1H) assay and complementary molecular experiments, we identified TuMYB46L that could bind to the promoter region of *TuACO3* and acted as a negative regulator of *TuACO3* expression. *TuMYB46L* was rapidly downregulated by *Bgt* infection, thus permitting enhanced expression of *TuACO3* in the infected plants. Therefore, *TuMYB46L* and *TuACO3* comprise a functional gene module that regulates ET biosynthesis to promote einkorn wheat defense against *Bgt*. We further identified four chitinase genes that function downstream of the *TuMYB46L-TuACO3* module through transcriptome comparison. Together, our data provide new information on the function of ET biosynthesis in wheat defense against *Bgt* and the transcriptional control of plant *ACO* gene in powdery mildew-infected plants.

Materials and Methods

Plant materials

The *Triticum urartu* accessions used in this work included PI428193, PI428202, PI428214, PI428220, PI428224 and G1812 (Zhang *et al.*, 2016; Ling *et al.*, 2018). They were all susceptible to the *Blumeria graminis* f.sp. *tritici* (*Bgt*) race E09. G1812 has previously been used for determining the genomic sequence of *T. urartu* (Ling *et al.*, 2018). The common wheat cultivar Kenong 199 (KN199), highly susceptible to E09 (Wang

et al., 2014; Zou *et al.*, 2018), was used for propagating *Bgt* and as a recipient for developing the transgenic wheat lines overexpressing *TuACO3* or *TuMYB46L* (ACO, 1-aminocyclopropane-1-carboxylic acid (ACC) oxidase; MYB, myeloblastosis).

Bgt infection and phenotyping

Wheat seeds were germinated in the glasshouse at 20–22°C under a 16 h : 8 h, light : dark photoperiod for 1 wk to yield seedlings at the one-leaf stage. They were inoculated with E09 spores as described by Wang *et al.* (2014). At 72 h post-inoculation (hpi), the leaves were cut into 5-cm segments, and subjected to microcolony staining using Coomassie blue (Wang *et al.*, 2014). For each inoculation, 10–15 leaves from ≥ 10 infected seedlings were examined, with the results used to calculate the percentage of microcolonies developing from the total number of examined *Bgt* spores. For observing the development of *Bgt* colonies, the infected leaves were photographed at 8 d post-inoculation (dpi), with *Bgt* colony area determined using ImageJ software (https://imagej.nih.gov/ij/).

Quantification of ethylene content

Ethylene (ET) content was measured using a gas chromatography instrument (Yin *et al.*, 2015). For the samples without *Bgt* inoculation, the seedlings (30 for *T. urartu* and 10 for common wheat) at the one-leaf stage were transferred into a 50-ml Falcon tube with their roots immersed in water. After 24 h at 22°C, the tube was tightly sealed with a rubber cap for 24 h, with the emitted ET subsequently measured. In the case of *Bgt* inoculation, the desired seedlings were placed into the Falcon tube, followed by *Bgt* inoculation as described above, with the tube sealed immediately post-inoculation. The ET content was measured at 24 hpi, and repeated three times, with each measurement including three biological replicates.

Gene expression analysis by qRT-PCR

Gene expression levels were determined using the samples collected from at least 10 seedlings (including untreated controls and those treated for 24 h) by quantitative reverse transcription (qRT)-PCR with gene-specific primers (Supporting Information Table S1; Methods S1).

Single-cell functional assay

Single-cell functional tests, based on transient overexpression (TOE) of cloned cDNA or transiently induced gene silencing (TIGS) in wheat epidermal cells, were accomplished essentially as described in previous publications (Douchkov *et al.*, 2005; Shen *et al.*, 2007). The reporter plasmid contained the expression cassette of β-glucuronidase gene. The effector constructs were pUbi:TuACO3, pUbi:TuMYB46L, pUbi:TuACO3as or pUbi:TuMYB46Las. The former two constructs transiently expressed the full-length cDNA of *TuACO3* and *TuMYB46L*, respectively, whereas the latter two plasmids contained a short segment from *TuACO3* or *TuMYB46L* coding sequence in an antisense orientation (Methods S1).

Immunoblotting assay

Immunoblotting was carried out using either the antibody to a recombinant TuACO3 protein or the FLAG tag (Sigma, F7425). The recombinant TuACO3 was prepared by expressing a histidine-tagged protein in *Escherichia coli*, with the purified protein used to raise a mouse polyclonal antibody as described by Qin *et al.* (2008). More details are described in Methods S1.

Virus-induced gene silencing

Virus-induced gene silencing (VIGS) was carried out using the barley stripe mosaic virus (BSMV) vector (Yuan *et al.*, 2011). Two constructs, pCaBS-γ:ACO3as and pCaBS-γ:MYB46Las harboring a short antisense fragment derived from the coding sequence of *TuACO3* (122 bp) or *TuMYB46L* (130 bp), were prepared. Together with pCaBS-α and pCaBS-β, the two recombinant viruses, BSMV:ACO3as and BSMV:MYB46Las, were formed, and used to silence endogenous *TuACO3* and *TuMYB46L* in G1812 leaf cells, respectively. The two viruses also were used to silence the orthologous genes of *TuACO3* or *TuMYB46L* in the common wheat cultivar KN199 because the VIGS-inducing fragments carried by BSMV:ACO3as and BSMV:MYB46Las were conserved in the respective orthologs (Methods S1).

Overexpression of *TuACO3* and *TuMYB46L* in common wheat

The constructs pUbi:TuACO3-FLAG and pUbi:TuMYB46L-FLAG, expressing TuACO3-FLAG and TuMYB46L-FLAG fusion proteins, respectively, were prepared with the vector pHZ206 (carrying a maize ubiquitin gene promoter) and the primers listed in Table S1. They were introduced into the immature embryos of KN199 by biolistic transformation (Wang *et al.*, 2014). Homozygous T_2 lines were selected from selfed T_1 individuals, with the expression of TuACO3-FLAG or TuMYB46L-FLAG identified by immunoblotting using the antibodies recognizing FLAG tag or TuACO3. In total, 12 and 17 independent lines overexpressing TuACO3-FLAG or TuMYB46L-FLAG were identified. TuACO3-OX1 and -OX2 (overexpressing TuACO3-FLAG) and TuMYB46L-OX1 and -OX2 (overexpressing TuMYB46L-FLAG) were used as representatives for more detailed analysis. These transgenic lines resembled wild-type (WT) KN199 in their growth and development in the glasshouse (Fig. S1). The transgenic plants and the WT segregate controls (WTS7 and WTS9) were inoculated with *Bgt*, followed by examination of microcolonies and colonies as detailed above. At least 30 plants were inoculated with *Bgt* per line per experiment. Measurement of ET content, either before or after *Bgt* inoculation, was carried out as described above. We were unable to overexpress *TuACO3* and

TuMYB46L in *T. urartu* because of the difficulty to genetically transform this species.

Yeast-one-hybrid (Y1H) assay

A Y1H library was generated using the vector pGADT7 and the SMART cDNA Library Construction Kit (634901; Clontech, Dalian, China). The cDNAs used for library construction were reverse-transcribed from total RNAs extracted from the G1812 leaves collected at 0, 4 and 24 hpi with *Bgt*. This library was screened using the 2-kb promoter region of *TuACO3* cloned in the bait vector pABAi (pABAi:TuACO3pro). The positive clones obtained from the initial screen were analyzed by DNA sequencing, with those carrying in frame inserts subjected to a second screen. To validate the binding of TuMYB46L to the *TuACO3* promoter region, the cDNA coding sequence of *TuMYB46L* was cloned into pGADT7, generating pGADT7:TuMYB46L. This construct was co-transformed with pABAi:TuACO3pro into the yeast strain Y1H Gold. Positive binding of TuMYB46L to *TuACO3* promoter region was indicated by abundant growth of the transformants on the SD/-Leu/-Ura/+AbA medium. As controls, pABAi:TuACO3mpro was prepared by mutating each of the four predicted MYB46 binding sites (E1–E4) within the 2-kb promoter region of *TuACO3* into AAAAAAA; pGADT7:EVC (empty vector control) and pGADT7:GFP (expressing green fluorescent protein, GFP) also were used to test the binding specificity (Methods S1).

Chromatin immunoprecipitation (ChIP)-quantitative (q) PCR analysis

Approximately 1×10^7 protoplasts, isolated according to Wang *et al.* (2014), were obtained from *c.* 150 G1812 seedlings. The pUbi:TuMYB46L-FLAG plasmid (20 μg) and the control vector pHZ206 (20 μg) (see above) each were transformed into *c.* 1×10^6 protoplasts using polyethylene glycol. After 18 h of culture in the dark, the protoplasts were collected and treated with 1% formaldehyde at room temperature for 15 min to promote protein-chromatin cross-linking (Bao *et al.*, 2014). The nuclei were then isolated, lysed and used for preparing chromatin complexes. The resulting complexes were ultrasonically treated to obtain a suitable input, in which the chromosomal DNA had been fragmented to a size of *c.* 500 bp, for ChIP. The anti-FLAG antibody (F7425; Sigma, Shanghai, China) was used to precipitate the chromatins, which were subsequently analyzed by qPCR with 20 different primer sets (Table S1) covering the 2-kb promoter region of *TuACO3*. As control, a mock precipitation with normal mouse IgG was executed. Two independent ChIP-qPCR experiments were performed with similar results obtained.

Electrophoretic mobility shift assay (EMSA)

The cDNA coding sequence of TuMYB46L was cloned into the pET-32a vector to express a recombinant TuMYB46L-HIS tag protein in the *E. coli* Rosetta (DE3) strain, which was purified to homogeneity using Ni-NTA Agarose (30210; Qiagen, Beijing, China). Three oligonucleotide probes (E1, E3 and E4, 39 bp each; Table S1) were synthesized and labeled with biotin at the 3′ end (Invitrogen, Beijing, China). An EMSA was performed using a LightShift Chemiluminescent EMSA kit (20148; Thermo Scientific, Beijing, China) according to the supplier's instructions. The biotin-labeled probes each were incubated in a reaction mixture (1 × binding buffer, 2.5% glycerol, 50 mM KCl, 5 mM $MgCl_2$, and 10 mM EDTA) with or without TuMYB46L protein at room temperature for 20 min. The following controls were included in the experiment to test the binding specificity: WT competitor (unlabeled E1, E3 and E4), mutant competitor (mutated and unlabeled E1, E3 and E4, with their MYB46 binding site changed to AAAAAAA, Table S1), and mutant probe (mutated and labeled E1, E3 and E4). The EMSA assay was carried out five times with identical findings made.

RNA sequencing and GO analysis of differentially regulated genes

Total RNA was extracted from the leaf samples collected from control G1812 seedlings and those treated with *Bgt* (at 24 hpi) or ET (at 24 h post-treatment). They were then subjected to RNA sequencing as reported by Dong *et al.*, (2015b). Three independent biological replicates were sequenced for each treatment at each time point. Two criteria were used to compute differentially expressed genes (DEGs), (1) a $\log_2$ ratio > 1.0 and (2) the expression difference was consistently observed in between different biological replicates. Gene ontology (GO) enrichment analysis of the DEGs shared by the two treatments was accomplished using the software AGRIGO (http://bioinfo.cau.edu.cn/agriGO/).

Analysis of chitinase genes and chitinase enzyme assay

The effects of ET treatment (10 ppm) or *Bgt* infection (for 24 h) on the expression of four chitinase genes were validated by qRT-PCR with gene-specific primers (Table S1). Transcript levels of the four genes in the G1812 leaf samples infected by BSMV:EVC, BSMV:ACO3as or BSMV:MYB46Las were evaluated by qRT-PCR. Total chitinase activities were assayed with a commercial kit (Solarbio, BC0820) following the manufacturer's guidelines (Methods S1).

Sequence information and raw data

Sequence information for *TuACO3*, *TuMYB46L*, *TaACO3*, *TaMYB46L*, VIGS-induced fragments and the DEGs identified by RNA sequencing, as well as the raw data used for calculating the means (± SE), are provided in Dataset S1.

Results

TuACO3 enhances wheat defense against *Bgt* via increasing ET biosynthesis

In our previous study (Zhang *et al.*, 2016), a gene encoding a putative ACO was found induced by *Bgt* infection in multiple

T. urartu accessions. This gene (*TuG1812G0600003491*), located on chromosome 6A of *T. urartu* (Ling *et al.*, 2018), is orthologous to rice *OsACO3* based on phylogenetic analysis (Fig. S2). Because of the poor understanding of ET function in plant defense against obligate biotrophic fungal pathogens and the fact that ACO catalyzes the last step of ET biosynthesis (Kende, 1993; Booker & Delong, 2015), we decided to analyze *TuACO3* further to gain insights into the function of ET in wheat defense against *Bgt*.

Using qRT-PCR, we validated the induction of *TuACO3* by *Bgt* in G1812 and another five diverse *T. urartu* accessions (Figs 1a, S3a). Immunoblot analysis revealed increased accumulation of native TuACO3 in G1812 leaf tissues at 24 hpi (Fig. 1b). Concomitant to this increase, ET production was significantly upregulated (by 50.2%) at 24 hpi (Fig. 1c). Similar rises of ET production were found in the other five *T. urartu* accessions at 24 hpi (Fig. S3b). In single-cell functional assays, *Bgt* infection level, as measured by the haustorium index, was decreased by overexpressing *TuACO3*, but uplifted by knocking down *TuACO3* expression via TIGS (Fig. 1d). Consistent with these findings, lowering *TuACO3* expression by BSMV-mediated VIGS decreased *Bgt* infection-induced ET production, and promoted susceptibility to *Bgt* in G1812 (Fig. 1e–h). Based on the reference genome sequence of Chinese Spring (CS) (International Wheat Genome Sequencing Consortium *et al.*, 2018), the orthologous gene of *TuACO3* in common wheat was *TraesCS6A02G325600* (*TaACO3*) (Fig. S3c). Silencing of this gene in the common wheat cultivar KN199 also increased the susceptibility to *Bgt* (Fig. S3d,e).

In order to further examine the function of *TuACO3* in ET biosynthesis and *Bgt* defense, we analyzed two independent common wheat transgenic lines (TuACO3-OX1, and -OX2) designed to overexpress TuACO3 with a C-terminal FLAG tag. In both lines, TuACO3-FLAG was confirmed to be overexpressed using immunoblotting with the antibodies to FLAG or TuACO3 (Fig. 2a). Compared to WTS7, a WT segregate control line, ET production was elevated by *c.* 1.7-fold in TuACO3-OX1 and 1.4-fold in TuACO3-OX2 (Fig. 2b). When infected by *Bgt*, the two OX lines showed significantly reduced fungal colonies on the leaf surface (Fig. 2c–f). These results demonstrated that the transgenically expressed TuACO3 functioned in ET biosynthesis, with concurrent improvement in *Bgt* defense.

The above findings prompted us to test if applying ET, or the chemicals known to stimulate or inhibit ET biosynthesis, may alter wheat defense against *Bgt* (Methods S1). This test was conducted using both G1812 and the common wheat variety KN199. Exogenous application of ET or ACC (a precursor of ET biosynthesis) significantly increased the resistance to *Bgt* in both G1812 and KN199, whereas the reverse was found when aminoethoxyvinylglycine (AVG, an inhibitor of ET biosynthesis) was applied (Fig. 3). The increased resistance against *Bgt* by exogenous ET was additionally confirmed using five more *T. urartu* accessions (Fig. S4). Together, the analyses presented above corroborate with each other, and suggest that *TuACO3*, induced by *Bgt* infection, promotes wheat defense against *Bgt* through significantly upregulating the content of ET.

TuMYB46L is a negative regulator of *TuACO3* expression

In order to identify the TF(s) controlling *Bgt* infection-induced expression of *TuACO3*, we screened a Y1H library using *TuACO3* promoter region as bait. This led to the identification of six genes whose proteins could bind to the promoter of *TuACO3* in two independent Y1H screens (Table S2). One of them, namely *TuMYB46L* (*TuG1812G0500001166*), was predicted to encode a MYB TF carrying a putative R2R3 MYB domain (Fig. S5a), whose full-length protein showed 35.2% identity to AtMYB46, a previously characterized MYB TF regulating secondary cell wall biosynthesis and host defense against *B. cinerea* in *Arabidopsis* (Zhong *et al.*, 2007; Ko *et al.*, 2009; Ramírez *et al.*, 2011a,b; Zhong & Ye, 2012; Kim *et al.*, 2014). Consistent with the identification of TuMYB46L by Y1H, the 2-kb promoter region of *TuACO3* was found to carry four *cis*-elements highly similar to the consensus binding site of AtMYB46, ACC(A/T)A(A/C)(T/C) (Zhong & Ye, 2012) (Fig. S5b). We therefore focused on analyzing the potential regulation of *TuACO3* transcription by TuMYB46L.

The specific binding of TuMYB46L to *TuACO3* promoter was verified by including additional controls (Fig. 4a). The binding was not observed when the four putative MYB46 recognition sites in the promoter region of *TuACO3* were all mutated to AAAAAAA; neither was it observed when free GFP was used as prey and WT *TuACO3* promoter region as bait. In the effector–promoter reporter assay conducted in *Nicotiana benthamiana* leaves, expression of TuMYB46L, but not free GFP, suppressed the promoter activity of *TuACO3* (Fig. 4b,c). TuMYB46L did not suppress the activity of the mutant promoter of *TuACO3* (with all four MYB46 recognition sites changed to AAAAAAA) as effectively as it did for the WT promoter of *TuACO3* (Fig. 4b, c). Phylogenetic analysis validated the relatedness of TuMYB46L to its homologs (including AtMYB46) from monocot and dicot plants (Fig. S5c). However, the predicted proteins of TuMYB46L and its close cereal homologs (ZmMYB46 and OsMYB46) were considerably larger than those of AtMYB46 and the homologs from dicot plants (Fig. S5c). As anticipated, TuMYB46L was targeted to the nucleus when transiently expressed as a YFP fusion protein in *N. benthamiana* leaf cells (Methods S1; Fig. S5d).

The expression of *TuMYB46L* was strongly and rapidly decreased by *Bgt* infection in all six *T. urartu* accessions examined (Fig. 4d). Silencing *TuMYB46L* expression by BSMV-mediated VIGS resulted in a significantly greater induction of *TuACO3* at 24 hpi of *Bgt*, and substantially more ET was produced in *TuMYB46L* silenced plants relative to their controls (Fig. 4e–g). The *Bgt* microcolonies recorded for *TuMYB46L* silenced plants were substantially fewer than those found for the controls (Fig. 4h,i). In agreement with these results, the defense against *Bgt* was compromised by overexpressing *TuMYB46L*, but strengthened after silencing *TuMYB46L* by TIGS, in the single-cell transfection assays conducted with *T. urartu* leaves (Fig. S6a, b). BSMV-mediated VIGS also was conducted for the orthologous gene of *TuMYB46L* in common wheat

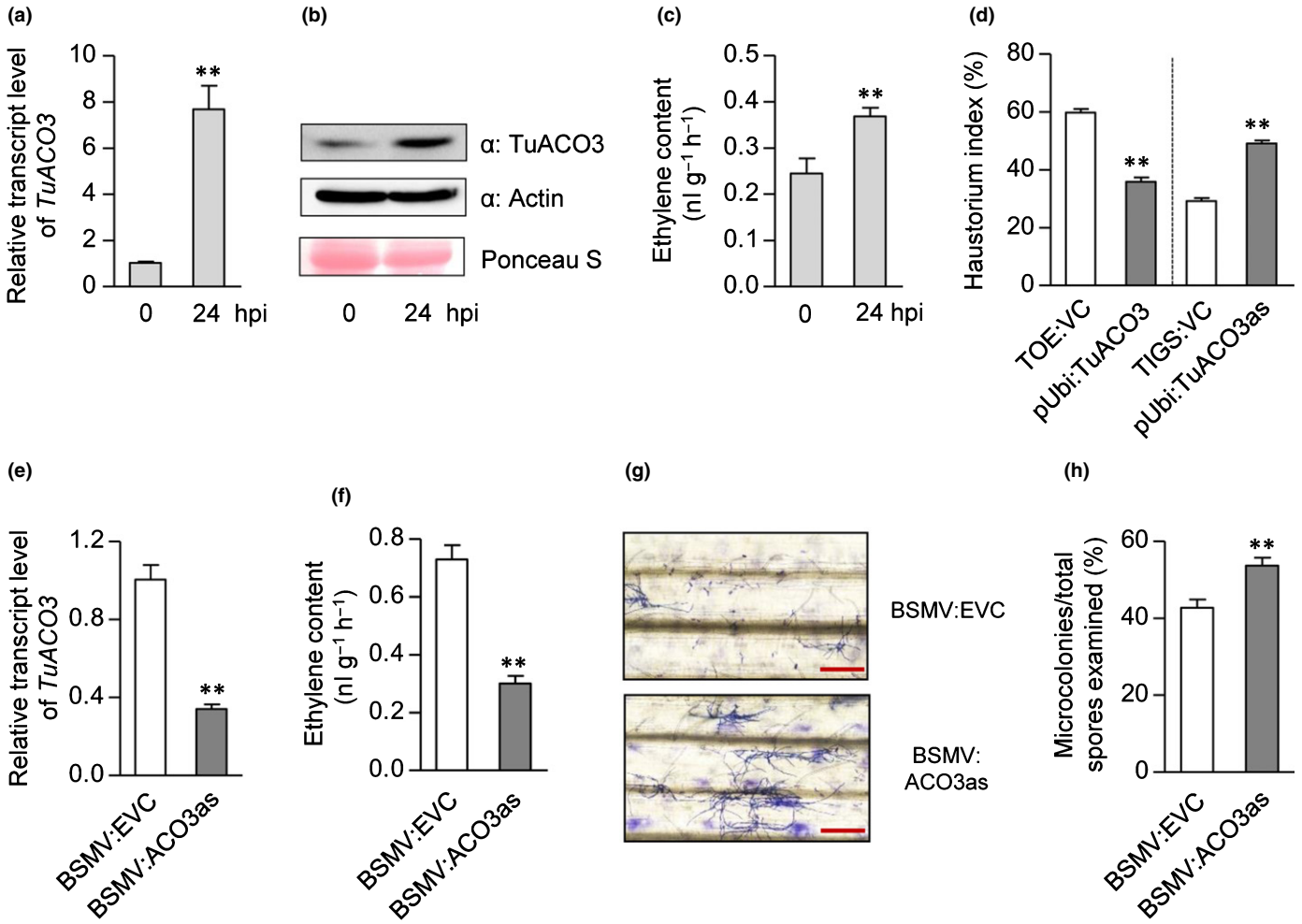

Fig. 1 Functional analysis of *TuACO3* in the *Triticum urartu* accession G1812. (a–c) Elevation of *TuACO3* expression and ethylene (ET) production at 24 h post-inoculation (hpi) of *Blumeria graminis* f.sp. *tritici* (*Bgt*). Transcript and protein increases were revealed by quantitative reverse transcription (qRT-PCR) (a) and immunoblotting with a *TuACO3*-specific antibody (b). Detection of actin served as an internal control. Upregulation of ET biosynthesis was determined by gas chromatography analysis (c). (d) *Bgt* haustorium growth in the leaf cells, suppressed by transiently expressing *TuACO3* from the construct pUbi:TuACO3 but stimulated by transiently silencing *TuACO3* with the construct pUbi:TuACO3as. TOE:VC and TIGS:VC, empty vector controls for the transient overexpression and silencing assays, respectively. Each mean (± SE) was calculated from the data of three technical repeats (with more than 200 transfected cells examined in each repeat). The results shown were typical of three independent experiments. **, $P < 0.01$ (Student's *t*-test). (e–h) Effects of silencing *TuACO3* on *Bgt* defense and ET production. Silencing was achieved using the recombinant virus BSMV:ACO3as. BSMV:EVC, an empty BSMV vector, served as a control. BSMV:ACO3as lowered the transcript level of *TuACO3* (e), decreased ET production (f), and increased the development of *Bgt* microcolonies as shown by Coomassie blue staining of fungal structures (g) and quantitative comparison with the control (h). The datasets presented each were representative of three independent experiments. Each mean (± SE) was calculated from at least three biological replicates. **, $P < 0.01$ (Student's *t*-test). Bars, 200 μm. ACO, 1-aminocyclopropane-1-carboxylic acid oxidase.

(*TraesCS5A02G101000*, *TaMYB46L*), which led to substantial increase of *TaACO3* transcript level and considerable decrease of the susceptibility to *Bgt* (Fig. S6d–f).

We further analyzed two independent transgenic lines (TuMYB46L-OX1 and TuMYB46L-OX2) overexpressing a TuMYB46L-FLAG tag protein in the common wheat cultivar KN199. Expression of TuMYB46L-FLAG in the transgenic lines was confirmed by immunoblotting (Fig. 5a). Infection with *Bgt* significantly upregulated ET production in WTS9, a corresponding WT segregate control line, but this upregulation was diminished in TuMYB46L-OX1 and TuMYB46L-OX2 (Fig. 5b). Consistently, substantially more *Bgt* microcolonies and stronger *Bgt* colony growth were observed on TuMYB46L-OX1 and TuMYB46L-OX2 leaves than on those of WTS9 (Fig. 5c–f). These findings, together with the foregoing results (Fig. 4), indicate that TuMYB46L is a negative regulator of *TuACO3* expression, and that its downregulation is required for the enhancement of *TuACO3* expression, ET content and *Bgt* defense in wheat.

TuMYB46L binds to *cis*-elements in the promoter region of *TuACO3*

Among the four putative MYB46 binding sites in the 2-kb sequence upstream of the initiation codon of *TuACO3*, the first one (E1, ACCAAAG) was located near the ATG codon, and the

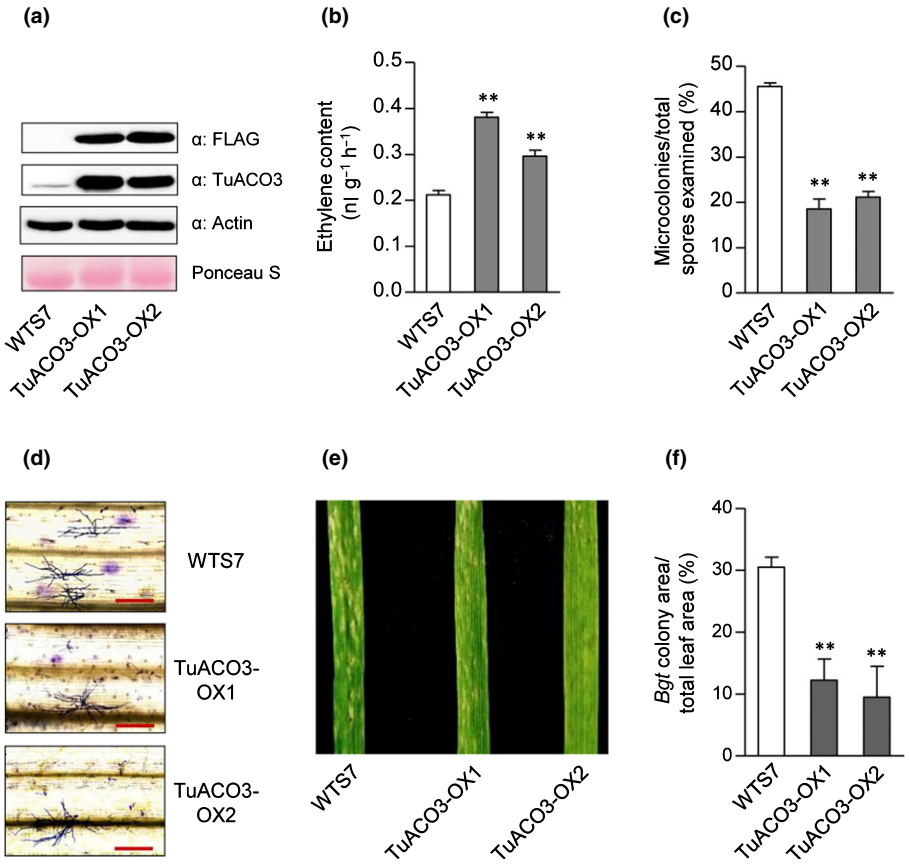

Fig. 2 Validation of *TuACO3* function using transgenic common wheat plants. TuACO3-OX1 and -OX2 were two independent representative homozygous transgenic lines. WTS7 was a wild-type (WT) segregate served as a control. (a) Overexpression of TuACO3-FLAG protein in TuACO3-OX1 and -OX2 revealed by immunoblotting with the antibodies specific for the FLAG tag or TuACO3. Equal loading was checked by detection of actin and Ponceau S staining. (b) Increased ethylene (ET) production in TuACO3-OX1 and -OX2 relative to WTS7. (c, d) Reduced development of *Blumeria graminis* f.sp. *tritici* (*Bgt*) microcolonies in TuACO3-OX1 and -OX2 recorded at 72 h post-inoculation (hpi), as shown by quantitative comparison with WTS7 (c) and Coomassie blue staining of fungal structures (d). (e, f) Differences in *Bgt* colony growth among WTS7 and TuACO3-OX1 and -OX2 at 8 d post-inoculation (dpi), as indicated by the photographs of *Bgt*-infected leaves (e) and quantitative comparison of the percentages of *Bgt* colony area. The datasets shown each were representative of at least three independent experiments. The numerical data shown were means ± SE, with those in (b) and (c) determined from three biological replicates. The means in (f) each were obtained by scanning nine *Bgt*-infected leaves from three separate experiments. **, $P < 0.01$ (Student's *t*-test). Bars, 200 μm. ACO, 1-aminocyclopropane-1-carboxylic acid oxidase.

third (E3, ACCTAAA) and fourth (E4, ATTTGGT) were more distant (Figs 6a, S5b). We first performed ChIP-qPCR assays to test the binding of TuMYB46L to different regions of *TuACO3* promoter. A TuMYB46L-FLAG tag protein was transiently expressed in *T. urartu* leaf protoplasts, followed by ChIP with the antibody against FLAG. Co-precipitating DNAs were quantified by qPCR using primer sets covering the 2 kb promoter. Compared to the control in which the FLAG antibody was replaced by normal mouse IgG, the inclusion of FLAG antibody led to the precipitation of substantially more DNA fragments carrying E1 or E3 + E4, but not that harboring E2, with the average enrichment obtained for the two regions being *c.* 3.5-fold and 2.3-fold, respectively (Fig. 6b).

We thus conducted EMSA to validate the binding of E1, E3 and E4 by a bacterially expressed, histidine-tagged TuMYB46L protein. As anticipated, the TuMYB46L-HIS tag protein was able to bind all three elements in repeated EMSA experiments (Fig. 6c). The binding was specific because it was not found with the mutant probes, it decreased by the WT competitor probes, but it was not affected by the mutated competitor probes (Fig. 6c).

Multiple processes and genes function in ET-mediated defense against *Bgt*

In order to gain insight into the biological processes and genes functioning in ET-mediated wheat defense against *Bgt*, we carried out two types of transcriptome assays. The first type used the G1812 leaf samples without or with *Bgt* inoculation for 24 h, and the second employed the G1812 leaves without or with ET treatment for 24 h. For *Bgt* treatment, the up- and down-regulated genes were 2307 and 1516, respectively; for ethylene treatment the differentially expressed genes were 1406 (up-regulated) and 1222 (down-regulated), respectively (Fig. 7a). The up-regulated and down-regulated genes shared by the two treatments amounted to 691 and 559, respectively (Fig. 7b). For the shared upregulated genes, the significantly enriched biological processes were related to chitin catabolism,

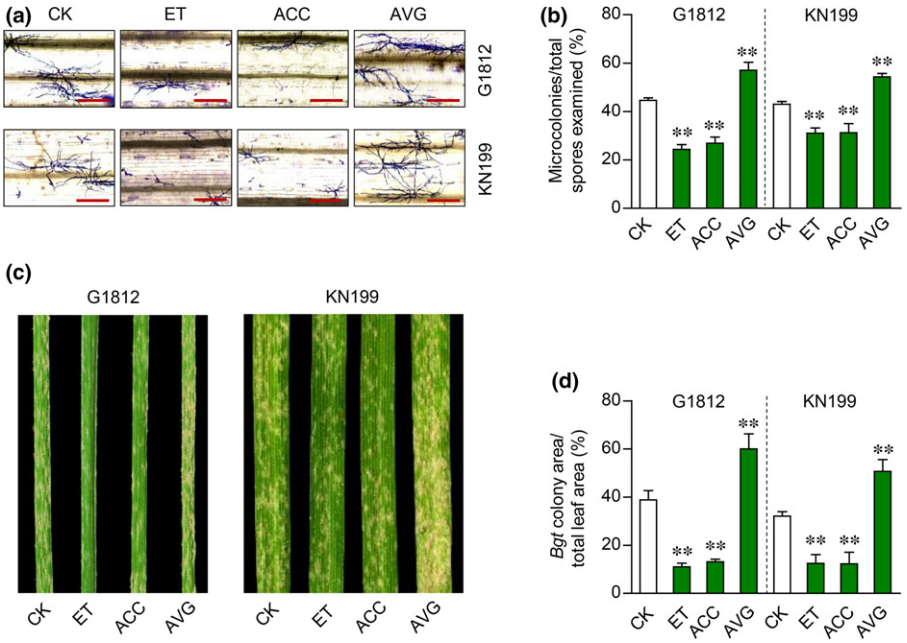

Fig. 3 Effect of changing ethylene (ET) concentration on *Blumeria graminis* f.sp. *tritici* (*Bgt*) defense in the *Triticum urartu* accession G1812 and the common wheat cultivar Kenong 199 (KN199). Ethylene (10 ppm) was applied by placing plants in sealed containers. 1-Aminocyclopropane-1- carboxylic acid (ACC, 20 μM) and aminoethoxyvinylglycine (AVG, 10 μM) were applied by spraying. The plants were inoculated with *Bgt* at 24 h after the treatment. (a, b) Influence of *Bgt* microcolony development by ET, ACC or AVG as revealed by Coomassie blue staining of fungal structures (a) and quantitative comparison with the control (CK) (b). The samples were analyzed at 72 h post-inoculation (hpi). (c, d) Differences in *Bgt* colony growth on the leaves treated by ET, ACC or AVG at 8 d post-inoculation (dpi), as shown by the photographs of *Bgt*-infected leaves (c) and quantitative comparison of the percentages of *Bgt* colony area (d). The data displayed were typical of four independent experiments. The means (± SE) in (b) each were calculated from eight seedlings; those in (d) each were obtained by scanning 12 *Bgt*-infected leaves from four separate experiments. **, $P < 0.01$ (Student's *t*-test). Bars, 200 μm.

cellulose biosynthesis and isoprenoid biosynthesis; for the shared downregulated genes, the highly enriched biological processes included oxidation reduction and metal ion transport (Table S3).

Because previous studies have shown the increase of host chitinase gene expression in fungal-infected plant tissues and the involvement of ET in the induction process (Jacobs *et al.*, 1999; Akagi *et al.*, 2011), we further analyzed the four chitinase genes (i.e., *TuG1812G0100002418*, *TuG1812G0200004053*, *TuG1812G0200004054* and *TuG1812G0300003072*, Ling *et al.*, 2018) that were upregulated by both *Bgt* and ET treatments (Table S4). The fold-induction of the four genes varied approximately from three to nine (after *Bgt* infection) or two to four (post ET application) (Table S4). Their upregulated expression after *Bgt* or ET treatment was confirmed by qRT-PCR (Fig. 7c). Importantly, the expression of the four chitinase genes all were repressed in the *T. urartu* leaf tissues in which *TuACO3* was silenced by BSMV-mediated VIGS, but promoted in those with downregulated *TuMYB46L* expression (Fig. 7d).

Consistent with the foregoing results, total chitinase activities were substantially elevated by *Bgt* infection (1.5-fold) or ET treatment (1.3-fold) in *T. urartu* (Fig. 7e). Moreover, total chitinase activity levels in the two *TuACO3* overexpression transgenic lines were significantly higher than that of the control (WTS7) (Fig. 7f). By contrast, total chitinase activities in the two *TuMYB46L* overexpression lines were substantially lower relative to those of the control WTS9 (Fig. 7f).

Discussion

In this work, we studied the functions of *TuACO3* and *TuMYB46L*, and discovered a previously uncharacterized gene module (i.e. *TuMYB46L-TuACO3*; ACO, 1-aminocyclopropane-1-carboxylic acid (ACC) oxidase; MYB, myeloblastosis) that regulates ethylene (ET) biosynthesis and content in einkorn wheat defense against *Blumeria graminis* f.sp. *tritici* (*Bgt*). The findings were made primarily in the einkorn wheat *Triticum urartu*, and subsequently confirmed in common wheat by barley stripe mosaic virus (BSMV)-mediated virus-induced gene silencing (VIGS) and using the KN199 transgenic lines overexpressing *TuACO3* or *TuMYB46L*.

The expression and function of *TuACO3* are enhanced in *Bgt*-infected wheat

Although ACO has long been known to catalyze the last step of ET biosynthesis (Spanu & Boller, 1989; Kende, 1993; Booker & DeLong, 2015), it is only recently that several studies have uncovered the importance of transcriptional control in the function of ACO during cotton fiber development, apple fruit ripening and *Arabidopsis* root development (Li *et al.*, 2014; T. Li *et al.*, 2017; Hu *et al.*, 2019; Park *et al.*, 2018) . A number of studies have recorded changes in the expression of various *ACO* gene members accompanying the infections by different pathogens (Shan & Goodwin, 2006; Yu *et al.*, 2011; Vilanova *et al.*, 2017),

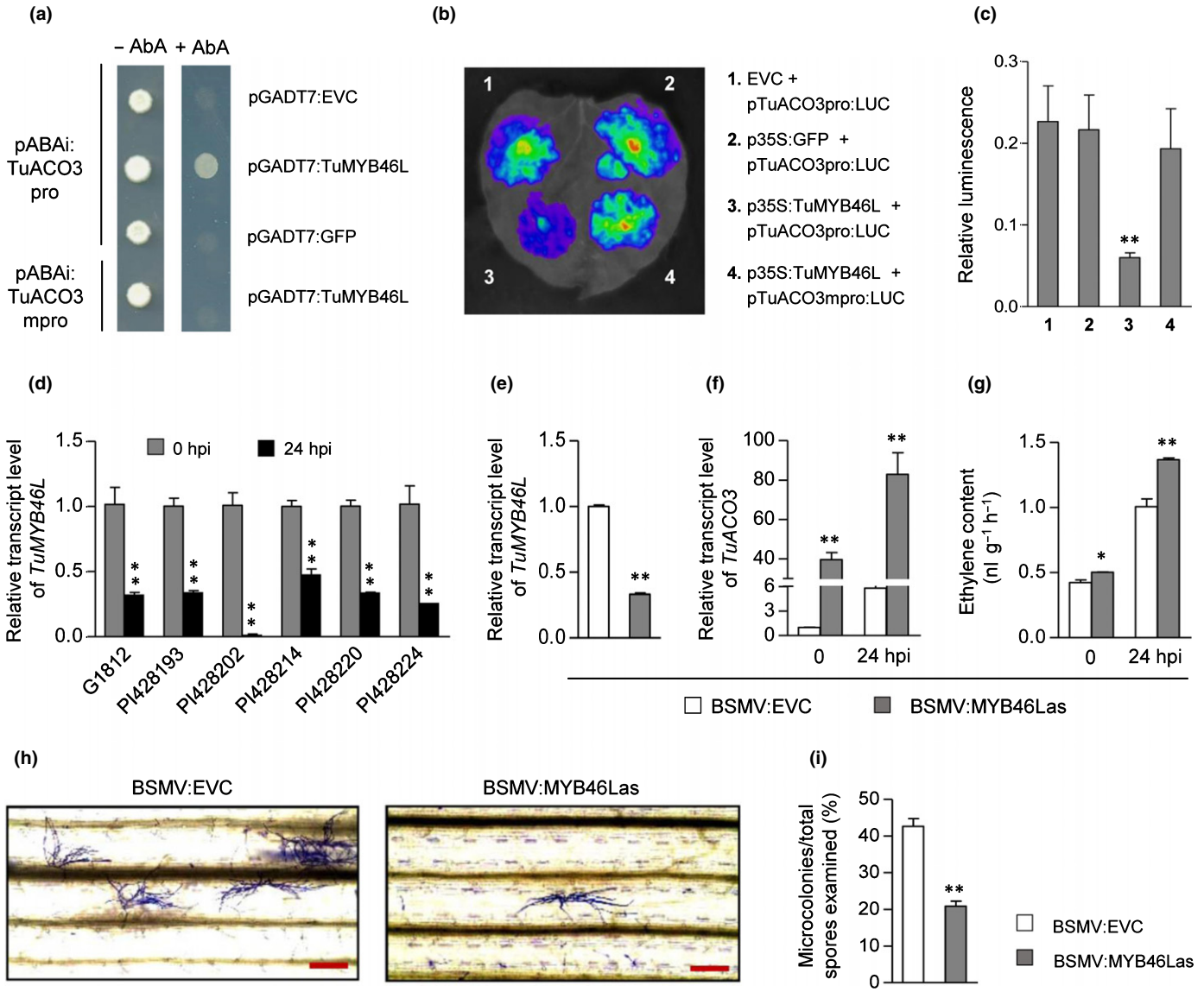

Fig. 4 Functional analysis of *TuMYB46L*. (a) Binding of TuMYB46L to *TuACO3* promoter of in yeast-one-hybrid (Y1H) assay. The constructs pABAi: TuACO3pro and pABAi:TuACO3mpro carried wild-type (WT) or mutated versions of *TuACO3* promoter (2 kb); the mutant was created by changing each of the four MYB46 recognition sites into AAAAAAA. The plasmids pGADT7:TuMYB46L and pGADT7:GFP expressed TuMYB46L or GFP. The plasmid pGADT7:EVC was used as empty vector control. Positive binding of TuMYB46L to the WT promoter of *TuACO3* was indicated by abundant growth of the yeast carrying both pABAi:TuACO3pro and pGADT7:TuMYB46L in the presence of aureobasidin A (AbA). (b, c) Suppression of *TuACO3* promoter (carried by pTuACO3pro:LUC) activity by TuMYB46L in *Nicotiana benthamiana* leaf cells, as evidenced by luminescence imaging (b) and quantitative comparison of luciferase signals (c). The luciferase signals specified by *TuACO3* promoter were strongly suppressed by TuMYB46L (expressed from p35S:TuMYB46L) but not by green fluorescent protein (GFP) (expressed from the control construct p35S:GFP). No suppression was obtained with the empty vector control (EVC). TuMYB46L did not suppress the activity of a mutant *TuACO3* promoter (carried in pTuACO3mpro:LUC, with all four MYB46 recognition sites changed to AAAAAAA) as effectively as it did for the WT promoter of *TuACO3*. (d) Decreased expression of *TuMYB46L* in six different *Triticum urartu* accessions at 24 h post inoculation (hpi) as detected by qRT-PCR. (e–i) BSMV mediated silencing of *TuMYB46L* in the *T. urartu* accession G1812. Compared to the empty viral vector control (BSMV:EVC), the recombinant virus BSMV:MYB46Las carrying the silencing-inducing fragment lowered *TuMYB46L* transcript level (e), and promoted *TuACO3* expression (f) and ethylene production (g) in both the control and *Blumeria graminis* f.sp. *tritici* (*Bgt*)-inoculated plants. *Bgt* microcolony development was strongly inhibited in the plants in which *TuMYB46L* was silenced as indicated by Coomassie blue staining of fungal structures (h) and quantitative comparison (i). The datasets shown each were representative of three independent experiments. Each mean (± SE) was determined from three biological replicates. *, $P < 0.05$; **, $P < 0.01$ (Student's *t*-test). Bars, 200 μm. ACO, 1-aminocyclopropane-1-carboxylic acid oxidase; MYB, myeloblastosis.

but the function of the concerned *ACO* and the underlying regulatory mechanism were generally not analyzed using molecular genetic means.

Based on the data gathered here, we suggest that the function of *TuACO3* is enhanced in *Bgt*-infected wheat, which contributes to host defense against *Bgt* via significantly increasing ET

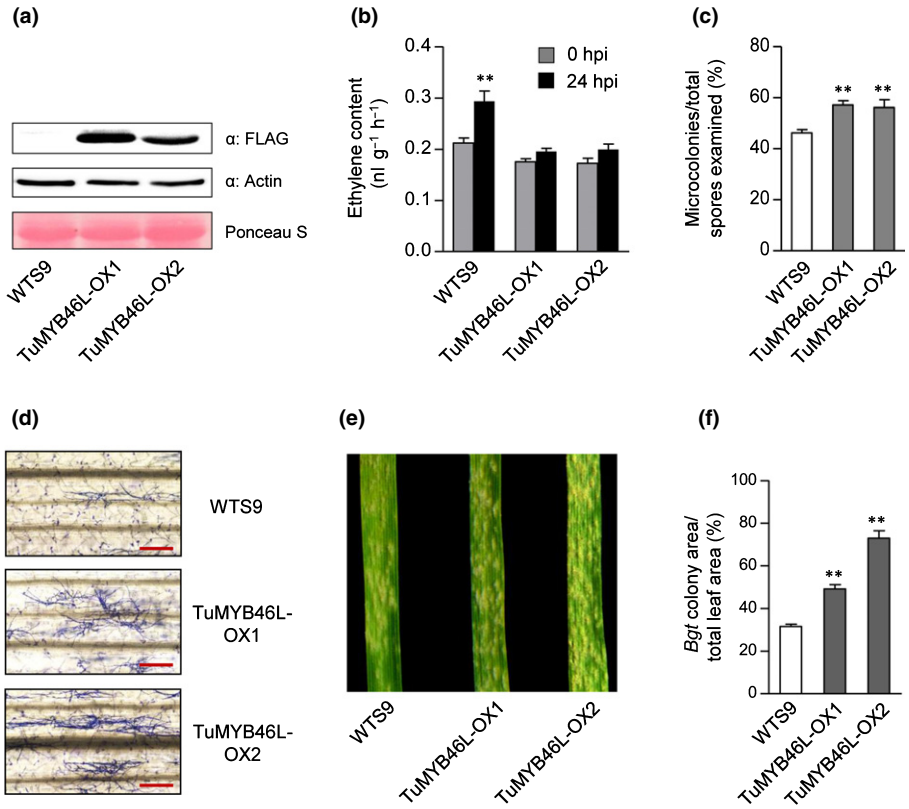

Fig. 5 Verification of *TuMYB46L* function using transgenic plants developed with the common wheat cultivar Kenong 199. TuMYB46L-OX1 and -OX2 were two independent representative homozygous transgenic lines. WTS9 was a wild-type (WT) segregate used as a control. (a) Overexpression of TuMYB46L-FLAG protein in TuMYB46L-OX1 and -OX2 revealed by immunoblotting with the antibody specific for FLAG. Detection of actin and staining by Ponceau S indicated equal loading. (b) Upregulation of ethylene biosynthesis by *Blumeria graminis* f.sp. *tritici* (*Bgt*) infection was depressed in TuMYB46L-OX1 and -OX2 but not in WTS9. (c, d) Increased development of *Bgt* microcolonies in TuMYB46L-OX1 and -OX2 at 72 h post-inoculation (hpi), as shown by quantitative comparison with WTS9 (c) and Coomassie blue staining of fungal structures (d). (e, f) Stronger *Bgt* colony growth observed in TuMYB46L-OX1 and -OX2 relative to that in WTS9 at 8 dpi, as indicated by the photographs of *Bgt*-infected leaves (e) and quantitative comparison of the percentages of *Bgt* colony area. The data displayed each were typical of three independent experiments. The means (± SE) in (b) and (c) each were calculated from three biological replicates; those in (f) each were obtained by scanning nine *Bgt*-infected leaves from three separate experiments. **, $P < 0.01$ (Student's *t*-test). Bars, 200 μm. MYB, myeloblastosis.

biosynthesis and content. Importantly, we validated the promotion of wheat defense against *Bgt* by *TuACO3* via elevating ET biosynthesis through analyzing two independent common wheat transgenic lines overexpressing *TuACO3* (Fig. 2). Thus, our work has generated molecular and functional evidence for the positive contribution of an *ACO* gene to plant defense against pathogen infection through elevating ET concentration.

Before this work, there has been some evidence for the involvement of ET in plant defense against powdery mildew fungi. The *Arabidopsis* mutant *cev1* displays constitutively active jasmonic acid/ET induced defense responses and shows increased resistance to three different powdery mildew pathogens (Ellis & Turner, 2001). In grapevine, powdery mildew infection and artificial treatment with ethephon induce an overlapping set of defense-related proteins (Jacobs *et al.*, 1999). The present work demonstrates that ET biosynthesis evidently is upregulated in *Bgt*-infected wheat and contributes to host defense against *Bgt*. Although this contribution did not offer a complete protection to the disease, it probably reduced disease severity because silencing *TuACO3* not only decreased ET production, but also increased the development of powdery mildew colonies in *Bgt*-infected wheat (Fig. 1e–h). Furthermore, we showed that exogenous application of ET enhanced wheat resistance to *Bgt* and that inhibition of ET biosynthesis by aminoethoxyvinylglycine (AVG) aggravated susceptibility to *Bgt* (Fig. 3). Consequently, our work suggests that ET-mediated defense can be activated by an adapted powdery mildew pathogen in a compatible interaction in wheat. This provides a new molecular insight into the role of ET in plant defense to biotrophic fungal pathogens.

Consistent with the increased *TuACO3* expression and ET production discussed above, the transcript level of one *1-aminocyclopropane-1-carboxylic acid synthase* (*ACS*) gene (i.e. *TuACS2*), which functions immediately upstream of *ACO* (Booker & DeLong, 2015), was elevated in *Bgt*-infected *T. urartu* plants (Fig. S7). The activity of *TuACS2* may enhance the generation of the precursor ACC for ET biosynthesis in *Bgt*-invaded wheat tissues. However, further work is needed to validate this possibility.

Because the *ACO* gene family is well conserved in higher plants (Booker & DeLong, 2015; Sun *et al.*, 2017; Park *et al.*, 2018), and powdery mildew diseases occur in diverse plant species (Glawe 2008), it is worth investigating whether the enhancement

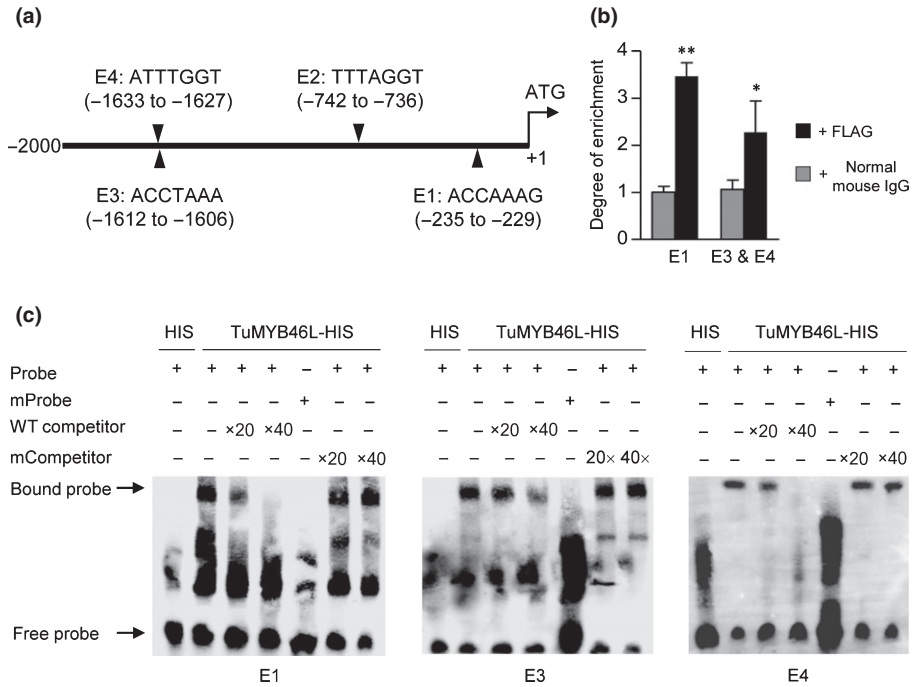

Fig. 6 Binding of TuMYB46L to *TuACO3* promoter region. (a) A diagram showing the positions of four putative MYB46 binding sites (E1–E4) in the 2-kb promoter region of *TuACO3*. (b) Chromatin immunoprecipitation-quantitative (ChIP-q)PCR assay. The assay was conducted by expressing a TuMYB46L-FLAG protein in G1812 leaf protoplasts, with the chromatins bound to TuMYB46L-FLAG precipitated using the FLAG antibody and subsequently quantified by qPCR. The chromatin fragments carrying the E1 element or harboring the closely spaced E3 and E4 elements were strongly enriched in the precipitation with FLAG antibody compared to the mock precipitation with normal mouse IgG. The means (± SE) each were calculated from three biological replicates, and statistically compared using Student's *t*-test. *, $P < 0.05$; **, $P < 0.01$. (c) Validation of the binding of TuMYB46L to E1, E3 and E4 by EMSA. A TuMYB46L-HIS protein expressed in *Escherichia coli* was purified; its binding to biotin-labeled E1, E3 or E4 probes was tested in the absence or presence of unlabeled wild-type (WT) probes. No specific binding was obtained with the labeled mutant probes in which the putative binding sites were all changed to AAAAAAA. Moreover, the specific binding of TuMYB46L-HIS to E1, E3 and E4 was not affected by the presence of the unlabeled mutant probes. Three sets of independent assays were performed, which all validated the binding of TuMYB46L-HIS to E1, E3 and E4. ACO, 1-aminocyclopropane-1-carboxylic acid oxidase; MYB, myeloblastosis.

of plant defense by *ACO*, as revealed here, also may happen in other powdery mildew pathosystems. Considering the limited understanding on most of the powdery mildew diseases recorded to date (Glawe 2008), molecular and functional analysis of *ACO* may provide a generally useful entry point for studying host defense mechanisms to different powdery mildew fungi.

Downregulation of *TuMYB46L* is required for elevated expression of *TuACO3* after *Bgt* infection

Judging from the molecular genetic data obtained (Figs 4, 5), we suggest that downregulation of *TuMYB46L* is a prerequisite for the elevated expression of *TuACO3* in *Bgt*-infected wheat and its subsequent function in increasing ET biosynthesis. Central to the action of TuMYB46L is its ability to bind to multiple *cis*-elements in the promoter region of *TuACO3* (Fig. 6). The rapid decline of *TuMYB46L* expression following *Bgt* infection diminishes the binding of its protein to the promoter of *TuACO3*, which permits transcriptional upregulation of *TuACO3* in *Bgt*-infected wheat. Thus, *TuMYB46L* is likely a negative regulator of *TuACO3* expression and function under normal growth conditions.

As a vital phytohormone, the biosynthesis of ET must be tightly regulated according the environmental conditions to which the plants are exposed (Booker & DeLong, 2015; Broekgaarden *et al.*, 2015). Failure to adjust ET biosynthesis and signaling lessens plant adaptation to harmful environments (Guo & Ecker, 2003; Booker & DeLong, 2015; Broekgaarden *et al.*, 2015). Therefore, *TuMYB46L* regulates ET biosynthesis through controlling the expression of *TuACO3* according to the presence or absence of *Bgt* infection in wheat. The significance of the *TuMYB46L-TuACO3* module in wheat defense against *Bgt* via regulating ET production is clearly demonstrated in this work. Further study is needed to examine if the negative regulation of *TuACO3* by *TuMYB46L* also may be required for efficient plant growth under normal environmental conditions.

Among the homologs of TuMYB46L (Fig. S5c), only AtMYB46 from *Arabidopsis* has so far been shown to affect plant response to pathogen challenge (Ramírez *et al.*, 2011a,b). The knockout plants of *AtMYB46* showed increased disease resistance to *Botrytis cinerea* because of changed cell wall integrity and more efficient induction of the genes involved in cell wall remodeling or pathogen defense than WT plants (Ramírez *et al.*, 2011a,b). In view of the relatedness of TuMYB46L to AtMYB46, on the one hand, it will be interesting to investigate if the contribution of the *TuMYB46L-TuACO3* module to wheat defense against *Bgt* also may involve changed cell wall integrity and enhanced expression of cell wall remodeling genes, in addition to the upregulation of *TuACO3* expression and ET production observed in

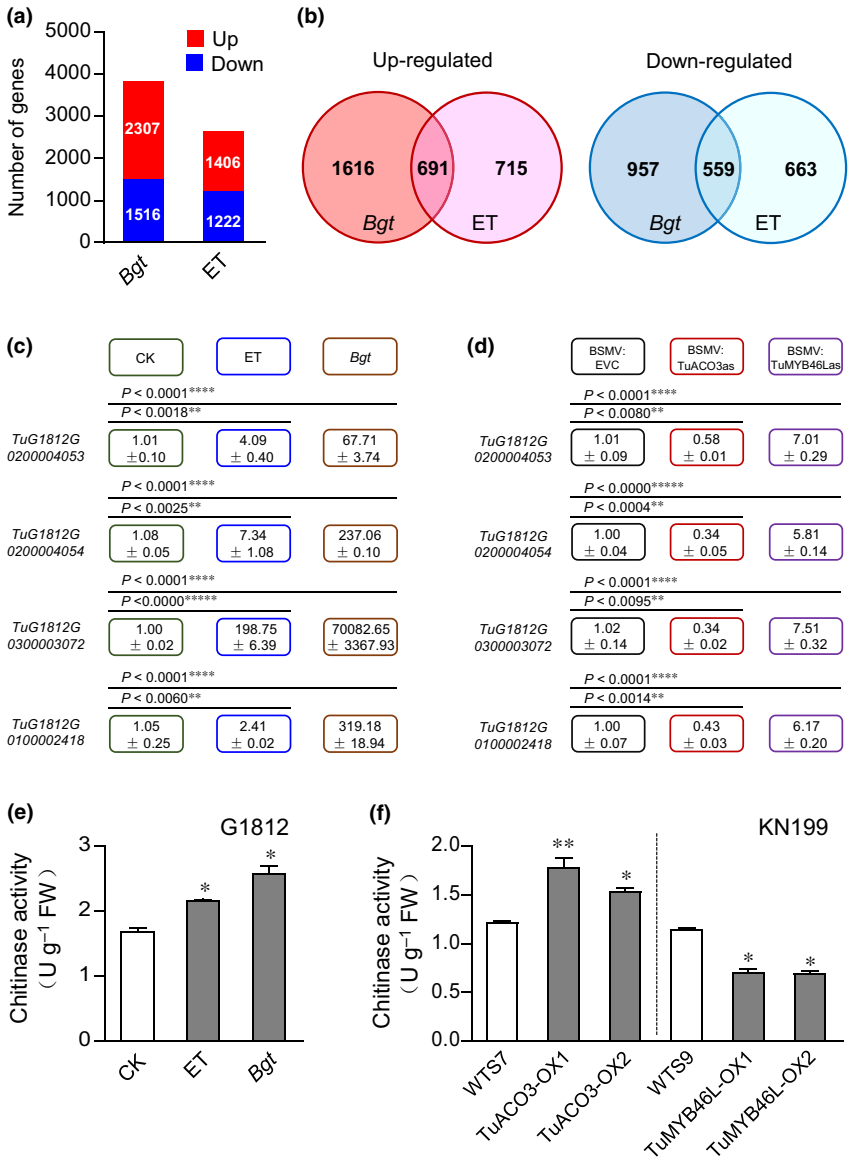

Fig. 7 Analysis of the genes regulated by *Blumeria graminis* f.sp. *tritici* (*Bgt*) inoculation and ethylene (ET) treatment. (a) The numbers of up- and downregulated genes triggered by *Bgt* inoculation or ET treatment in the *Triticum urartu* accession G1812. (b) The numbers of up- and downregulated genes shared by *Bgt* inoculation and ET treatment. (c) Validation by quantitative reverse transcription (qRT)-PCR of the four chitinase genes upregulated by *Bgt* inoculation and ET treatment, with the obtained relative expression values shown in the color-coded boxes. The actual significance levels as compared to the control (CK) also were displayed. (d) Effects of silencing *TuACO3* or *TuMYB46L* on the expression of four chitinase genes. Transcript levels of the four genes in the G1812 plants inoculated with BSMV-EVC (empty vector control), BSMV:ACO3as (silencing *TuACO3*), or BSMV:MYB46Las (silencing *TuMYB46L*) were evaluated by qRT-PCR with gene-specific primers. The relative expression values scored were indicated in the color-coded boxes, and the actual significance levels as compared to the control (BSMV:EVC) also were provided. (e) Elevation of total chitinase activities in the G1812 plants treated by ET or *Bgt* inoculation compared to the untreated controls (CK). The samples used for the assay were collected at 24 h after ET (10 ppm) treatment or at 24 h post-inoculation (hpi) of *Bgt*. (f) Total chitinase activities were increased in the transgenic lines overexpressing *TuACO3* (TuACO3-OX1 and -OX2), but decreased in the other two transgenic lines overexpressing *TuMYB46L* (TuMYB46L-OX1 and -OX2) relative to their corresponding WTS controls. In (c) to (f), the data presented were representative of three independent experiments, with each mean (± SE) calculated from three biological replicates. *, $P < 0.05$; **, $P < 0.01$; ***, $P < 0.001$; ****, $P < 0.0001$; *****, $P < 0.00001$ (Student's *t*-test). ACO, 1-aminocyclopropane-1-carboxylic acid oxidase; MYB, myeloblastosis.

this work. On the other hand, it also may be worthwhile to investigate the potential existence of an *AtMYB46-AtACO* module and its possible contribution to *Arabidopsis* defense against pathogens. In a preliminary analysis, we found that AtMYB46 could suppress the promoter activity of *AtACO4*, which is the closest *Arabidopsis* homolog of *TuACO3* (65.8% protein identity), and that the promoter region of *AtACO4* also carries five predicted AtMYB46 binding sites (Fig. S8). Whether the suppression of *AtACO4* promoter activity by AtMYB46 may take part in the regulation of *AtACO4* transcription during *Arabidopsis* pathogen defense is an important question for future research. Also important for future study is to examine if

TuMYB46L may regulate secondary cell wall development as this is a shared function among MYB46 homologs (Zhong *et al.*, 2011; Xie *et al.*, 2018); TuMYB46L may resemble AtMYB46 and the MYB46 homolog from birch in being able to regulate multiple plant processes (Ramírez *et al.*, 2011a,b; Guo *et al.*, 2017). Nevertheless, certain functional difference between TuMYB46L and AtMYB46 is to be expected because the identity level of their full-length proteins (35.2%) is not high and their proteins differ substantially in size (Fig. S5a,c).

The relationships among ET biosynthesis and signaling, cell wall development, organ growth and pathogen defense are very complex, and may involve growth–defense trade-offs (Ramírez *et al.*, 2011a,b; Souza *et al.*, 2017; Xie *et al.*, 2018). The finding of the participation of an *Arabidopsis* ACS protein (ACS5) in cell wall biosynthesis independent of ET concentration adds further complexity to the interactions (Xu *et al.*, 2008). However, we demonstrated here that the *TuMYB46L-TuACO3* module increased ET production in *Bgt*-infected wheat, and that exogenous application of ET or ACC enhanced wheat defense against *Bgt*. Thus, further research on the *TuMYB46L-TuACO3* module may help to improve understanding of the interplays among ET biosynthesis and signaling, cell wall development and function, plant growth and pathogen defense.

Chitinase genes participate in ET-mediated defense against *Bgt*

Through transcriptome comparison and validation by quantitative reverse-trancription (qRT)-PCR, the expression of four different chitinase genes was confirmed to be upregulated by both *Bgt* infection and ET treatment (Fig. 7a–c; Table S4). Furthermore, the four genes were depressed by silencing *TuACO3* but elevated after suppressing *TuMYB46L* (Fig. 7d), suggesting that they act downstream of the *TuACO3-TuMYB46L* module. This proposition is additionally supported by (1) increased total chitinase activities in the wheat plants infected by *Bgt* or treated with ET (Fig. 7e) and in those overexpressing *TuACO3* (Fig. 7f), and (2) reduced total chitinase activities in the wheat lines overexpressing *TuMYB46L* (Fig. 7f).

Plant chitinase isozymes are potent players in host defense against fungal pathogens (Pusztahelyi, 2018), and past studies have reported the involvement of ET in the induction of host chitinase gene expression in fungal-infected plants (Jacobs *et al.*, 1999; Akagi *et al.*, 2011). This work improves the understanding of chitinase gene induction by a pathogenic fungus (*Bgt*) through identifying a specific host gene module (*TuMYB46L-TuACO3*) that produces the endogenous ET signal needed for the induction. The next challenge is to reveal how ET orchestrates chitinase gene expression. In this context, it is interesting to note that overexpression of certain ET responsive factors (ERFs) can enhance the expression of pathogenesis-related proteins including chitinase (Berrocal-Lobo *et al.*, 2002; Akagi *et al.*, 2011; Zhu *et al.*, 2014). It also will be interesting to test if reactive oxygen species (ROS) and additional pathogenesis-related genes may be involved in the defense processes regulated by *TuMYB46L-TuACO3* in further research.

Apart from chitinase genes, our transcriptome analysis also detected upregulation of the genes involved in the biosynthesis of cellulose or isoprenoids in *Bgt*-infected or ET-treated wheat plants (Table S3). On the one hand, there is now increasing evidence that alterations in cellulose biosynthesis and cell wall integrity modulate plant defense against pathogens (Caño-Delgado *et al.*, 2003; Hernández-Blanco *et al.*, 2007; Souza *et al.*, 2017). On the other, the phytoalexins derived from phenylpropanoid metabolism are active defense compounds against plant pathogens (Ahuja *et al.*, 2012; Liu *et al.*, 2015). Therefore, elevated expression of the genes functioning in cellulose or isoprenoid biosynthesis may help to strengthen the defense against *Bgt* in wheat. We noted that the 2-kb promoter region of the three upregulated cellulose synthase genes, as well as the two upregulated phenylalanine ammonia lyase genes, each carried two or three putative MYB46 binding sites (Table S5). We are now in the process of investigating if these genes also may be regulated by the *TuMYB46L-TuACO3* module.

In summary, this study establishes that the *TuMYB46L-TuACO3* module regulates ET biosynthesis to promote einkorn wheat defense against *Bgt*. The insights obtained improve our knowledge on wheat defense mechanisms to *Bgt* and on the ACO enzyme that is critical in generating the ET signal for plant adaptation to changing environment (Booker & DeLong, 2015). Our work points to the possibility of controlling wheat powdery mildew disease through manipulating ET concentration, and may stimulate further research into the regulation and function of ET biosynthesis in plant defense against diverse powdery mildew fungi.

Acknowledgements

This study was supported by the key research and development program of the Ministry of Science and Technology of the People's Republic of China (2016YFD0101004, 2017YFD0100600). We thank Mingyue Gou for constructive suggestions on manuscript preparation. The RNA-Seq data generated in this study were deposited in the Genome Sequence Archive of Beijing Institute of Genomics (accession no. CRA001335).

Author contributions

HZ, KZ and DW designed the project; HZ, LD and XH performed the experiments; HZ, LD, HJ and CY performed the analyses; KZ, YH, BL, HQ, QS and JZ contributed to data collection; and HZ and DW wrote the manuscript. HZ and LD contributed equally to this work.

ORCID

Lingli Dong https://orcid.org/0000-0003-1990-9559
Xinyun Han https://orcid.org/0000-0003-2037-2592
Yali Han https://orcid.org/0000-0002-3721-5609
Bei Li https://orcid.org/0000-0002-4569-0768
Huanju Qin https://orcid.org/0000-0003-1899-9150

Qianhua Shen https://orcid.org/0000-0002-9446-3086
Daowen Wang https://orcid.org/0000-0002-6230-8735
Kunpu Zhang https://orcid.org/0000-0002-1561-916X
Hongyuan Zheng https://orcid.org/0000-0002-3000-8703

References

Ahuja I, Kissen R, Bones AM. 2012. Phytoalexins in defense against pathogens. *Trends in Plant Science* **17**: 73–90.

Akagi A, Dandekar AM, U Stotz H. 2011. Resistance of *Malus domestica* fruit to *Botrytis cinerea* depends on endogenous ethylene biosynthesis. *Phytopathology* **101**: 1311–1321.

Al-Attala MN, Wang X, Abou-Attia MA, Duan X, Kang Z. 2014. A novel TaMYB4 transcription factor involved in the defence response against *Puccinia striiformis* f. sp. *tritici* and abiotic stresses. *Plant Molecular Biology* **84**: 589–603.

Bao Z, Zhang N, Hua J. 2014. Endopolyploidization and flowering time are antagonistically regulated by checkpoint component MAD1 and immunity modulator MOS1. *Nature Communications* **5**: 5628.

Berrocal-Lobo M, Molina A, Solano R. 2002. Constitutive expression of ETHYLENE-RESPONSE-FACTOR1 in *Arabidopsis* confers resistance to several necrotrophic fungi. *The Plant Journal* **29**: 23–32.

Bigeard J, Colcombet J, Hirt H. 2015. Signaling mechanisms in pattern-triggered immunity (PTI). *Molecular Plant* **8**: 521–539.

Booker MA, DeLong A. 2015. Producing the ethylene signal: regulation and diversification of ethylene biosynthetic enzymes. *Plant Physiology* **169**: 42–50.

Broekaert WF, Delaure SL, De Bolle MF, Cammue BP. 2006. The role of ethylene in host-pathogen interactions. *Annual Review of Phytopathology* **44**: 393–416.

Broekgaarden C, Caarls L, Vos IA, Pieterse C, van Wees S. 2015. Ethylene: traffic controller on hormonal crossroads to defense. *Plant Physiology* **169**: 2371–2379.

Bhullar NK, Zhang Z, Wicker T, Keller B. 2010. Wheat gene bank accessions as a source of new alleles of the powdery mildew resistance gene *Pm3*: a large scale allele mining project. *BMC Plant Biology* **10**: 88.

Caño-Delgado A, Penfield S, Smith C, Catley M, Bevan M. 2003. Reduced cellulose synthesis invokes lignification and defense responses in *Arabidopsis thaliana*. *The Plant Journal* **34**: 351–362.

Cheng HQ, Han LB, Yang CL, Wu XM, Zhong NQ, Wu JH, Wang FX, Wang HY, Xia GX. 2016. The cotton MYB108 forms a positive feedback regulation loop with CML11 and participates in the defense response against *Verticillium dahliae* infection. *Journal of Experimental Botany* **67**: 1935–1950.

Chezem WR, Memon A, Li FS, Weng JK, Clay NK. 2017. SG2-Type R2R3-MYB transcription factor MYB15 controls defense-induced lignification and basal immunity in *Arabidopsis*. *Plant Cell* **29**: 1907–1926.

Cui H, Tsuda K, Parker JE. 2015. Effector-triggered immunity: from pathogen perception to robust defense. *Annual Review Plant Biology* **66**: 487–511.

Dong L, Cheng Y, Wu J, Cheng Q, Li W, Fan S, Jiang L, Xu Z, Kong F, Zhang D *et al.* 2015a. Overexpression of GmERF5, a new member of the soybean EAR motif-containing ERF transcription factor, enhances resistance to *Phytophthora sojae* in soybean. *Journal of Experimental Botany* **66**: 2635–2647.

Dong L, Liu H, Zhang J, Yang S, Kong G, Chu JS, Chen N, Wang D. 2015b. Single-molecule real-time transcript sequencing facilitates common wheat genome annotation and grain transcriptome research. *BMC Genomics* **16**: 1039.

Douchkov D, Nowara D, Zierold U, Schweizer P. 2005. A high-throughput gene-silencing system for the functional assessment of defense-related genes in barley epidermal cells. *Molecular Plant–Microbe Interactions* **18**: 755–761.

Ellis C, Turner JG. 2001. The *Arabidopsis* mutant *cev1* has constitutively active jasmonate and ethylene signal pathways and enhanced resistance to pathogens. *Plant Cell* **13**: 1025–1033.

Glawe DA. 2008. The powdery mildews: a review of the world's most familiar (yet poorly known) plant pathogens. *Annual Review of Phytopathology* **46**: 27–51.

Gravino M, Savatin DV, Macone A, De Lorenzo G. 2015. Ethylene production in *Botrytis cinerea*- and oligogalacturonide-induced immunity requires calcium-dependent protein kinases. *The Plant Journal* **84**: 1073–1086.

Guan R, Su J, Meng X, Li S, Liu Y, Xu J, Zhang S. 2015. Multilayered regulation of ethylene induction plays a positive role in *Arabidopsis* resistance against *Pseudomonas syringae*. *Plant Physiology* **169**: 299–312.

Guo H, Ecker JR. 2003. Plant responses to ethylene gas are mediated by SCF (EBF1/EBF2)-dependent proteolysis of EIN3 transcription factor. *Cell* **115**: 667–677.

Guo H, Wang Y, Wang L, Hu P, Wang Y, Jia Y, Zhang C, Zhang Y, Zhang Y, Wang C *et al.* 2017. Expression of the MYB transcription factor gene *BplMYB46* affects abiotic stress tolerance and secondary cell wall deposition in *Betula platyphylla*. *Plant Biotechnology Journal* **15**: 107–121.

He H, Zhu S, Zhao R, Jiang Z, Ji Y, Ji J, Qiu D, Li H, Bie T. 2018. *Pm21*, encoding a typical CC-NBS-LRR protein, confers broad-spectrum resistance to wheat powdery mildew disease. *Molecular Plant* **11**: 879–882.

Hernández-Blanco C, Feng DX, Hu J, Sanchez-Vallet A, Deslandes L, Llorente F, Berrocal-Lobo M, Keller H, Barlet X, Sanchez-Rodriguez C *et al.* 2007. Impairment of cellulose synthases required for *Arabidopsis* secondary cell wall formation enhances disease resistance. *Plant Cell* **19**: 890–903.

Hückelhoven R, Panstruga R. 2011. Cell biology of the plant-powdery mildew interaction. *Current Opinion in Plant Biology* **14**: 738–746.

Hu DG, Yu JQ, Han PL, Xie XB, Sun CH, Zhang QY, Wang JH, Hao YJ. 2019. The regulatory module MdPUB29-MdbHLH3 connects ethylene biosynthesis with fruit quality in apple. *New Phytologist* **221**: 1966–1982.

International Wheat Genome Sequencing Consortium (IWGSC), Appels R, Eversole K, Stein N, Feuillet C, Keller B, Rogers J, Pozniak CJ , Choulet F, Distelfeld A *et al.* 2018. Shifting the limits in wheat research and breeding using a fully annotated reference genome. *Science* **361**: pii: eaar7191.

Jacobs AK, Dry IB, Robinson SP. 1999. Induction of different pathogenesis-related cDNAs in grapevine infected with powdery mildew and treated with ethephon. *Plant Pathology* **48**: 325–336.

Kende H. 1993. Ethylene biosynthesis. *Annual Review of Plant Physiology and Plant Molecular Biology* **44**: 283–307.

Kim WC, Kim JY, Ko JH, Kang H, Han KH. 2014. Identification of direct targets of transcription factor MYB46 provides insights into the transcriptional regulation of secondary wall biosynthesis. *Plant Molecular Biology* **85**: 589–599.

Ko JH, Kim WC, Han KH. 2009. Ectopic expression of MYB46 identifies transcriptional regulatory genes involved in secondary wall biosynthesis in *Arabidopsis*. *The Plant Journal* **60**: 649–665.

Li F, Fan G, Wang K, Sun F, Yuan Y, Song G, Li Q, Ma Z, Lu C, Zou C *et al.* 2014. Genome sequence of the cultivated cotton *Gossypium arboreum*. *Nature Genetics* **46**: 567–572.

Li T, Xu Y, Zhang L, Ji Y, Tan D, Yuan H, Wang A. 2017a. The jasmonate-activated transcription factor MdMYC2 regulates ethylene responsive factor and ethylene biosynthetic genes to promote ethylene biosynthesis during apple fruit ripening. *Plant Cell* **29**: 1316–1334.

Li W, Zhu Z, Chern M, Yin J, Yang C, Ran L, Cheng M, He M, Wang K, Wang J *et al.* 2017b. A natural allele of a transcription factor in rice confers broad-spectrum blast resistance. *Cell* **170**: 114–126.

Ling HQ, Ma B, Shi X, Liu H, Dong L, Sun H, Cao Y, Gao Q, Zheng S, Li Y *et al.* 2018. Genome sequence of the progenitor of wheat A subgenome *Triticum urartu*. *Nature* **557**: 424–428.

Liu J, Osbourn A, Ma P. 2015. MYB transcription factors as regulators of phenylpropanoid metabolism in plants. *Molecular Plant* **8**: 689–708.

McNally KE, Menardo F, Lüthi L, Praz CR, Müller MC, Kunz L, Ben-David R, Chandrasekhar K, Dinoor A, Cowger C *et al.* 2018. Distinct domains of the $AVRPM3^{A2/F2}$ avirulence protein from wheat powdery mildew are involved in immune receptor recognition and putative effector function. *New Phytologist* **218**: 681–695.

Park CH, Roh J, Youn JH, Son SH, Park JH, Kim SY, Kim TW, Kim SK. 2018. *Arabidopsis* ACC oxidase 1 coordinated by multiple signals mediates ethylene biosynthesis and is involved in root development. *Molecules and Cells* **41**: 923–932.

Pieterse CM, Van der Does D, Zamioudis C, Leon-Reyes A, Van Wees SC. 2012. Hormonal modulation of plant immunity. *Annual Review of Cell and Developmental Biology* **28**: 489–521.

Pusztahelyi T. 2018. Chitin and chitin-related compounds in plant-fungal interactions. *Mycology* **9**: 189–201.

Qin C, Qian W, Wang W, Wu Y, Yu C, Jiang X, Wang D, Wu P. 2008. GDP-mannose pyrophosphorylase is a genetic determinant of ammonium sensitivity in *Arabidopsis thaliana*. *Proceedings of the National Academy of Sciences, USA* **105**: 18308–18313.

Ramírez V, Agorio A, Coego A, Garcia-Andrade J, Hernandez MJ, Balaguer B, Ouwerkerk PB, Zarra I, Vera P. 2011a. MYB46 modulates disease susceptibility to *Botrytis cinerea* in *Arabidopsis*. *Plant Physiology* **155**: 1920–1935.

Ramírez V, García-Andrade J, Vera P. 2011b. Enhanced disease resistance to *Botrytis cinerea* in *myb46 Arabidopsis* plants is associated to an early down-regulation of CesA genes. *Plant Signaling & Behavior* **6**: 911–913.

Shan XC, Goodwin PH. 2006. Silencing an ACC oxidase gene affects the susceptible host response of *Nicotiana benthamiana* to infection by *Colletotrichum orbiculare*. *Plant Cell Reports* **25**: 241–247.

Shen QH, Saijo Y, Mauch S, Biskup C, Bieri S, Keller B, Seki H, Ülker B, Somssich IE, Schulze-Lefert P. 2007. Nuclear activity of MLA immune receptors links isolate-specific and basal disease-resistance responses. *Science* **315**: 1098–1103.

Singh RP, Singh PK, Rutkoski J, Hodson DP, He X, Jorgensen LN, Hovmoller MS, Huerta-Espino J. 2016. Disease impact on wheat yield potential and prospects of genetic control. *Annual Review of Phytopathology* **54**: 303–322.

Spanu P, Boller T. 1989. Ethylene biosynthesis in tomato plants infected by *Phytophthora infestans*. *Journal of Plant Physiology* **134**: 533–537.

Souza CA, Li S, Lin AZ, Boutrot F, Grossmann G, Zipfel C, Somerville SC. 2017. Cellulose-derived oligomers act as damage-associated molecular patterns and trigger defense-like responses. *Plant Physiology* **173**: 2383–2398.

Sun X, Li Y, He W, Ji C, Xia P, Wang Y, Du S, Li H, Raikhel N, Xiao J *et al.* 2017. Pyrazinamide and derivatives block ethylene biosynthesis by inhibiting ACC oxidase. *Nature Communications* **8**: 15758.

Tintor N, Ross A, Kanehara K, Yamada K, Fan L, Kemmerling B, Nürnberger T, Tsuda K, Saijo Y. 2013. Layered pattern receptor signaling via ethylene and endogenous elicitor peptides during *Arabidopsis* immunity to bacterial infection. *Proceedings of the National Academy of Sciences, USA* **110**: 6211–6216.

Vilanova L, Vall-llaura N, Torres R, Usall J, Teixidó N, Larrigaudière C, Giné-Bordonaba J. 2017. *Penicillium expansum* (compatible) and *Penicillium digitatum* (non-host) pathogen infection differentially alter ethylene biosynthesis in apple fruit. *Plant Physiology and Biochemistry* **120**: 132–143.

Wang Y, Cheng X, Shan Q, Zhang Y, Liu J, Gao C, Qiu JL. 2014. Simultaneous editing of three homoeoalleles in hexaploid bread wheat confers heritable resistance to powdery mildew. *Nature Biotechnology* **32**: 947–951.

Wei X, Shan T, Hong Y, Xu H, Liu X, Zhang Z. 2017. TaPIMP2, a pathogen-induced MYB protein in wheat, contributes to host resistance to common root rot caused by *Bipolaris sorokiniana*. *Scientific Reports* **7**: 1754.

Wicker T, Oberhaensli S, Parlange F, Buchmann JP, Shatalina M, Roffler S, Ben-David R, Dolezel J, Simkova H, Schulze-Lefert P *et al.* 2013. The wheat powdery mildew genome shows the unique evolution of an obligate biotroph. *Nature Genetics* **45**: 1092–1096.

Xie M, Zhang J, Tschaplinski TJ, Tuskan GA, Chen JG, Muchero W. 2018. Regulation of lignin biosynthesis and its role in growth-defense tradeoffs. *Frontier in Plant Science* **9**: 1427.

Xing L, Di Z, Yang W, Liu J, Li M, Wang X, Cui C, Wang X, Wang X, Zhang R *et al.* 2017. Overexpression of ERF1-V from *Haynaldia villosa* can enhance the resistance of wheat to powdery mildew and increase the tolerance to salt and drought stresses. *Frontiers in Plant Science* **8**: 1948.

Xing L, Hu P, Liu J, Witek K, Zhou S, Xu J, Zhou W, Gao L, Huang Z, Zhang R *et al.* 2018. *Pm21* from *Haynaldia villosa* encodes a CC-NBS-LRR protein conferring powdery mildew resistance in wheat. *Molecular Plant* **11**: 874–878.

Xu SL, Rahman A, Baskin TI, Kieber JJ. 2008. Two leucine-rich repeat receptor kinases mediate signaling, linking cell wall biosynthesis and ACC synthase in *Arabidopsis*. *Plant Cell* **20**: 3065–3079.

Yahiaoui N, Srichumpa P, Dudler R, Keller B. 2004. Genome analysis at different ploidy levels allows cloning of the powdery mildew resistance gene *Pm3b* from hexaploid wheat. *The Plant Journal* **37**: 528–538.

Yang C, Li W, Cao J, Meng F, Yu Y, Huang J, Jiang L, Liu M, Zhang Z, Chen X *et al.* 2017. Activation of ethylene signaling pathways enhances disease resistance by regulating ROS and phytoalexin production in rice. *The Plant Journal* **89**: 338–353.

Yin CC, Ma B, Collinge DP, Pogson BJ, He SJ, Xiong Q, Duan KX, Chen H, Yang C, Lu X *et al.* 2015. Ethylene responses in rice roots and coleoptiles are differentially regulated by a carotenoid isomerase-mediated abscisic acid pathway. *Plant Cell* **27**: 1061–1081.

Yu M, Shen L, Zhang A, Sheng J. 2011. Methyl jasmonate-induced defense responses are associated with elevation of 1-aminocyclopropane-1-carboxylate oxidase in *Lycopersicon esculentum* fruit. *Journal of Plant Physiology* **168**: 1820–1827.

Yuan C, Li C, Yan L, Jackson AO, Liu Z, Han C, Yu J, Li D. 2011. A high throughput barley stripe mosaic virus vector for virus induced gene silencing in monocots and dicots. *PLoS ONE* **6**: e26468.

Zhang J, Zheng H, Li Y, Li H, Liu X, Qin H, Dong L, Wang D. 2016. Coexpression network analysis of the genes regulated by two types of resistance responses to powdery mildew in wheat. *Scientific Reports* **6**: 23805.

Zhong R, Lee C, McCarthy RL, Reeves CK, Jones EG, Ye ZH. 2011. Transcriptional activation of secondary wall biosynthesis by rice and maize NAC and MYB transcription factors. *Plant Cell Physiology* **52**: 1856–1871.

Zhong R, Richardson EA, Ye ZH. 2007. The MYB46 transcription factor is a direct target of SND1 and regulates secondary wall biosynthesis in *Arabidopsis*. *Plant Cell* **19**: 2776–2792.

Zhong R, Ye ZH. 2012. MYB46 and MYB83 bind to the SMRE sites and directly activate a suite of transcription factors and secondary wall biosynthetic genes. *Plant Cell Physiology* **53**: 368–380.

Zhu X, Qi L, Liu X, Cai S, Xu H, Huang R, Li J, Wei X, Zhang Z. 2014. The wheat ethylene response factor transcription factor pathogen-induced ERF1 mediates host responses to both the necrotrophic pathogen *Rhizoctonia cerealis* and freezing stresses. *Plant Physiology* **164**: 1499–1514.

Zou S, Wang H, Li Y, Kong Z, Tang D. 2018. The NB-LRR gene *Pm60* confers powdery mildew resistance in wheat. *New Phytologist* **218**: 298–309.

Supporting Information

Additional Supporting Information may be found online in the Supporting Information section at the end of the article.

Dataset S1 Sequence information and raw data.

Fig. S1 Morphology of transgenic wheat lines overexpressing TuACO3 or TuMYB46L.

Fig. S2 Phylogenetic analysis of ACO genes from different plant species.

Fig. S3 Elevation of *TuACO3* expression and ET production by *Bgt* infection in five different *T. urartu* accessions and analysis of *TaACO3* function in common wheat using BSMV-mediated VIGS.

Fig. S4 Inhibition of *Bgt* colony development and growth by ET treatment in five different *T. urartu* accessions.

Fig. S5 Primary structure, phylogeny and nuclear localization of *TuMYB46L* and predicted MYB46 binding sites in the 2-kb promoter region of *TuACO3*.

Fig. S6 Effects of transiently overexpressing or silencing *TuMYB46L* on *Bgt* haustorium growth and analysis of *TaMYB46L* function by VIGS in common wheat.

Fig. S7 Elevation of *TuACS2* transcript level by *Bgt* infection at 24 hpi.

Fig. S8 Suppression of *AtACO4* promoter activity by *AtMYB46*.

Methods S1 Additional description of methods.

Table S1 PCR primers used in this study.

Table S2 List of six *T. urartu* genes found in two independent Y1H screens.

Table S3 Significantly enriched biological processes identified by GO analysis.

Table S4 Expression changes of the four chitinase genes upregulated by both ET treatment and *Bgt* infection.

Table S5 Presence of putative MYB46 recognition sites in the 2-kb promoter region of the five genes related to cellulose or isoprenoid synthesis.

Please note: Wiley Blackwell are not responsible for the content or functionality of any Supporting Information supplied by the authors. Any queries (other than missing material) should be directed to the *New Phytologist* Central Office.